REAL-TIME HYPERSPECTRAL IMAGING WITH VOLUME HOLOGRAPHIC OPTICAL ELEMENTS

*Wenhai Liu, Demetri Psaltis**

California Institute of Technology
Department of Electrical Engineering
Mail-Stop 136-93
Pasadena, CA 91125

Arnab Sinha, George Barbastathis†

Massachusetts Institute of Technology
Department of Mechanical Engineering
Room 3-461c, 77 Massachusetts Ave.
Cambridge, MA 02139

ABSTRACT

We report a novel hyperspectral optical sensor capable of providing image information with four degrees of freedom (4D), *i.e.* volumetric spatial information and spectral information simultaneously, in real time. The imaging principle is based on the diffraction properties of volume holographic optical elements designed as spatial-spectral filters. The 4D imager can be configured to image objects in spatial scales ranging from meters to micrometers. The imager also enables feature matching in all four dimensions, which improves the information-extraction capabilities from the image data. We report experimental results and theoretical estimates on the image quality attainable by the 4D imager.

1. INTRODUCTION

Imaging in three-dimensional (3D) spaces is fundamentally an ill-posed problem, since detector arrays are necessarily two-dimensional. Several imaging techniques, e.g. confocal microscopy [1, 2], optical coherence tomography [3], coherence imaging [4, 5, 6, 7, 8], etc. resolve the ill-posedness by limiting the 3D field of view (by use of a pinhole in the first case and by decoherence in the next two) and scanning across the 3D object. Recently, the use of volume holograms as 3D imaging elements was proposed, first in the context of super-resolving confocal microscopy [9] and subsequently in more general contexts [10, 11]. Volume holographic imaging systems capture spectral information from volumetric objects due to the spectral degeneracy properties of volume holograms [10]. Thus, the hologram forms a map from the 4D (3D spatial +1D spectral) object space to the 2D detector, as shown in Figure 1.

*Supported by the National Science Foundation through the Neuromorphic Systems Engineering Research Center at Caltech and the Defense Advanced Research Projects Agency, Micro-Technology Office (MTO).
E-mail {wliu,psaltis}@optics.caltech.edu
†Supported by the National Science Foundation through the CAREER Award to G.B. and the Air Force Research Laboratories, Munitions Division (AFRL/MNK) Eglin AFB. E-mail: {arnab,gbarb}@mit.edu

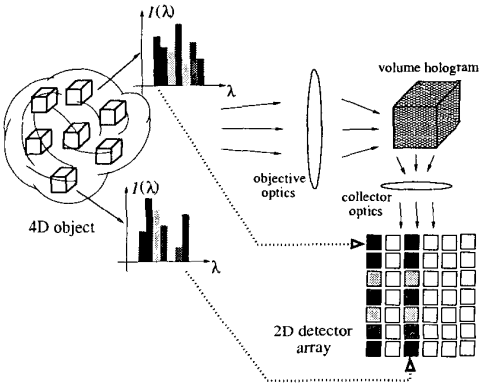

Fig. 1. Schematic diagram of the 4-D (volumetric spatial +spectral) image sensor using volume holography.

The object→image mapping properties of the volume hologram are also explained by virtue of the matched filter behavior of volume holograms with respect to their input illumination, which is well known from the contexts of holographic storage and optical pattern recognition. In other words, a volume hologram, unlike thin diffractive elements, does not diffract indiscriminately; among all components of a complex illuminating beam, significant scattering is produced only by those that yield phase-matched diffraction along the entire length of the volume hologram. Thus, matched filtering of the field input to the hologram is achieved by virtue of the Bragg matching process. Bragg matching along the spatial dimensions forms the basis of image correlators [12, 13] as well as angle and shift multiplexed [14, 15] holographic memories. Bragg matching in the spectral dimension forms the basis of wavelength multiplexing [14]. The connection of matched filtering to imaging and its implementation with volume holograms are central to the work described in this paper.

0-7803-6725-1/01/$10.00 ©2001 IEEE

2. VOLUME HOLOGRAPHIC IMAGING PRINCIPLES

The 4D imaging sensor is a specifically designed volume holographic element which acts as the principal imaging device, complemented with auxiliary optics and a planar optoelectronic detector. The principle of operation is shown in Figure 1. The objective optics transform the input field so that its physical dimensions match those of the volume hologram. The Bragg-matching properties of the hologram make it possible to distinguish wavefronts originating from different positions in 3-D space and at different wavelengths. The hologram separates light emitted from the object into channels according to source location and wavelength band. The separated light channels are four-dimensional resolution elements that we call *texels*. The hologram, through the collector optics, diffracts the light originating from each individual texel towards a different detector element at the output plane of the system. In this way, the 4-D input object is mapped unambiguously onto the 2-D detector surface. The number of unambiguous texels in the 4-D object space is equal to the smallest among the number of detector elements and the number of degrees of freedom in the response of the 3-D holographic element. The proposed method does not require any mechanical scanning; it provides single-shot capture and it can be compactly integrated into any imaging instrument (telescopes and microscopes are the most interesting.)

The texel-selective property described above can be generalized to the matching of more complicated spatial-spectral object signatures in scenes. Examples are the shape and absorption spectrum of large (wavelength-sized) particles before and after a particular chemical reaction, and the thermal signature of a fighter plane as function of location in its hull. In many applications, such signatures are known *a priori*. A volume-holographic imaging system with the signature recorded in the volume hologram as template is then a feature-specific imaging system which produces images of selected features only, ignoring the rest of the scene.

For example, consider a volume hologram recorded by a reference point source and a plane wave signal beam. The geometry is shown in Figure 2(a). Information about the location and wavelength of the reference is recorded in the orientation and spacing of the 3-D interference fringes. First suppose that the hologram is probed by a point source identical to the recording reference in both location and wavelength. The probing field will perfectly match the 3-D fringes and will produce a strong diffracted plane wave, *i.e.* it will be Bragg-matched. A point receiver placed in the Fourier plane of the recording signal beam (dashed line in Fig. 2a) will record maximum intensity. If the probe source is displaced with respect to the recording source but at the same wavelength, then in general the probe field does not perfectly match the 3-D fringes, and the diffracted field vanishes. An exception occurs along the out-of-plane $\hat{\mathbf{y}}$ direction, along which the fringes are invariant. (For this reason, the $\hat{\mathbf{y}}$ direction is called *degenerate*.) Therefore, if the probe source is an object extended around the location of the original recording source but at the same wavelength, then the only portion of the source that will produce significant diffraction is a thin line oriented along $\hat{\mathbf{y}}$. That Bragg-matched portion of the source will form a line image at the Fourier plane of the signal beam. The remaining portion of the extended probe passes through the hologram without diffracting in the direction of the signal beam. The matched imaging of the degenerate line is shown in Figure 2(b). Note that the above description is valid if the extended probe source is spatially incoherent, as most natural objects are. For partially coherent objects, the discriminating ability of the volume hologram along the $\hat{\mathbf{z}}$ direction is decreased.

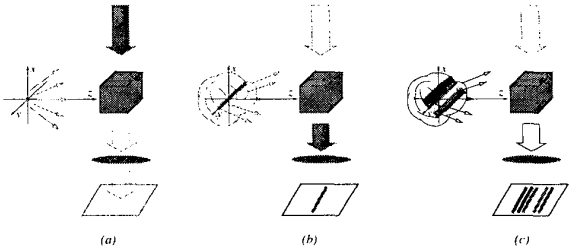

Fig. 2. Principle of operation of the volume holographic 4-D image sensor. (a) Recording of a volume hologram with a point-source reference beam and a plane-wave signal beam. (b) The same hologram images a line oriented along the $\hat{\mathbf{y}}$ direction when probed by an extended probe object source at the same wavelength as the recording reference. (c) The same hologram extracts a slice out of an extended polychromatic probe object.

Now suppose that the hologram is probed with an extended source which is also polychromatic (hyper-spectral.) In that case, in addition to the $\hat{\mathbf{y}}$-matching described above at the reference source wavelength, the 3-D interference fringes can be matched by portions of the source that are simultaneously at a different wavelength and $\hat{\mathbf{z}}$ position relative to the reference point source. Matching occurs when the combined wavelength-depth change results in identical 3-D interference fringes with the signal. Each wavelength-depth matched portion extends along a $\hat{\mathbf{y}}$-oriented line, together forming a slice across the probe. We refer to this matched slice as the *degeneracy surface* of the volume hologram. This matching portion of the probe is imaged onto a 2-D detector surface, whereas the remaining portion of the probe illumination passes through the hologram without

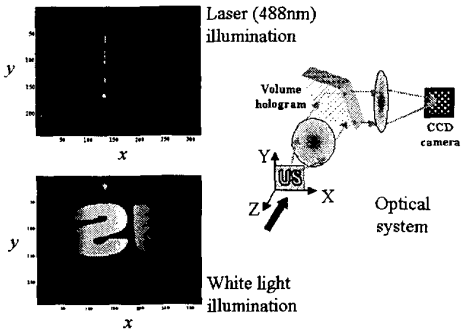

Fig. 3. An extended planar object imaged using the volume holographic system (the experimental arrangement is shown on the right). An opaque slide with the letters "US" in transmission is illuminated with a laser beam ($\lambda = 488$nm) and with white light. The laser image is the mono-chromatic $\hat{\mathbf{y}}$ degeneracy line discussed in the text. The white light image appears like a rain-bow composed of adjacent $\hat{\mathbf{y}}$ degeneracy lines at progressive colors.

diffracting, as shown in Figure 2(c). Thus, this single hologram recorded by a reference point source extracts a slice of the probe.

3. RESULTS

We have constructed experimental proof-of-principle demonstrations of volume holographic spectral microscopy. The imaging system consists of a single volume hologram recorded in the transmission geometry with a spherical wave transformed to a planar reference wave with an objective lens, and a plane wave signal beam at the Ar^+ line $\lambda =$ 488nm. Figures 3-4 show spectral imaging experiments with simple transparent objects illuminated with the recording Ar^+ laser line and with white light. The spatial-spectral selectivity of the hologram is demonstrated in the case of single laser-line illumination, whereas white line illumination creates rainbow images due to the holographic degeneracies discussed above.

We also performed imaging experiments using as object fluorescent microspheres with diameter 15μm embedded in polymer gel, which are excited by the same Ar^+ laser at 488nm. Different types emit fluorescence at peak wavelengths 505-515nm through 715-720nm as shown in the spectra of Figure 5. In Figure 6, a thicker host polymer allowed the beads to be arranged in two layers. The volume holographic imaging system exhibited superior selectivity in both depth and spectral dimensions compared to the regular microscope which was superimposed in the same experimental arrangement.

Preliminary numerical calculations of resolution, expressed as texel volume $\Delta x \times \Delta y \times \Delta z \times \Delta\lambda$, show that

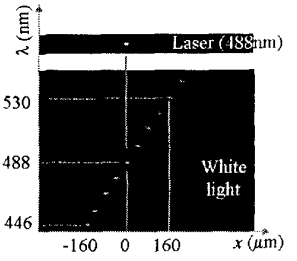

Fig. 4. Volume holographic image of a pinhole moving in the $\hat{\mathbf{x}}$ direction and illuminated with laser light (top) at the recording wavelength $\lambda = 488$nm of the hologram, and white light (bottom). The white pinhole produces images of progressively changing color as it moves along $\hat{\mathbf{x}}$. The laser-illuminated pinhole produces a single image at the center of the detector and disappears when it moves laterally.

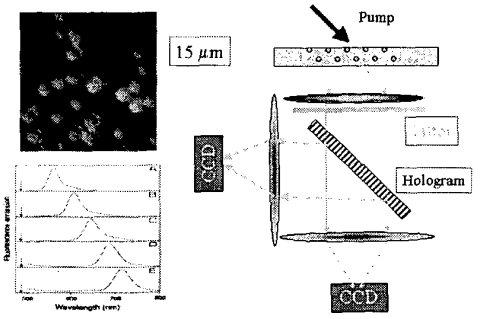

Fig. 5. Left: nominal spectra of the class of fluorescent beads used in our experiments (from `http://www.probe.com`). Right: schematic of the experimental volume holographic imaging arrangement which allows a bright-field microscope and a volume holographic microscope to be operated simultaneously.

the 4D imager can perform equally well or even outperform standard imaging elements. In a microscopy set-up and for modest hologram volumes (thickness of 0.5mm, aperture 2.5m and mid-visible wavelength operation at $\lambda_c = 500$nm) yield typical texel volumes of order 3μm $\times$ 3μm $\times$ 1μm $\times$ 0.25nm at a relatively limited field of view (300μm at distance $z_c = 2.5$mm). Our experimental arrangement with a 2mm thick polymer and a $\times 40$ objective is currently capable of $\Delta x = 2.6\mu$m, $\Delta z = 20 \sim 50\mu$m, and $\Delta\lambda = 0.16$nm. For telescopic systems the theoretical resolution scales proportionally to z_c in the lateral dimensions $\hat{\mathbf{x}}$, $\hat{\mathbf{y}}$ and proportionally to z_c^2 inthe longitudinal dimension $\hat{\mathbf{z}}$. Exact optimization of the trade-offs between field of view, magnification, and resolution is among the objectives of our ongoing research.

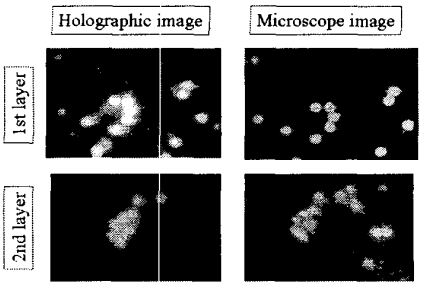

Fig. 6. Volume holographic image of two layers of fluorescent beads at different wavelengths. The experimental arrangement is the same as in Figure 5. The volume holographic images on the left exhibit both depth and spectral selectivity. The microscope images on the right exhibit limited depth selectivity only (out-of-focus layers appear as uniform background.)

4. DISCUSSION

We presented a novel imaging technique based on diffraction of light from volume holograms. Our preliminary results verify the capability of volume holographic imaging systems to acquire slice-by-slice images of quasi-transparent objects while simultaneously separating their spectral components. The next steps in our research are the experimental demonstrations of real-time imaging in all four dimensions simultaneously as well as correlation of spatial-spectral features in *a priori* known objects.

5. REFERENCES

[1] M. Minsky, "Microscopy apparatus," US Patent 3,013,467, granted 1961.

[2] T. Wilson, Ed., *Confocal microscopy*, Academic Press, 1990.

[3] D. Huang, E. A. Swanson, C. P. Lin, J. S. Schuman, W. G. Stinson, W. Chang, M. R. Hee, T. Flotte, K. Gregory, C. A. Puliafito, and J. G. Fujimoto, "Optical coherence tomography," *Science*, vol. 254, no. 5035, pp. 1178–1181, 1991.

[4] R. N. Bracewell, "Radio astronomy techniques," in *Encyclopaedia of physics*, S. Flügge, Ed., vol. 54. Springer-Verlag, 159.

[5] W. H. Carter and E. Wolf, "Correlation theory of wavefields generated by fluctuating, three-dimensional, primary, scalar sources I. General theory," *Opt. Acta*, vol. 28, pp. 227–244, 1981.

[6] K. Itoh and Y. Ohtsuka, "Fourier-transform spectral imaging: retrieval of source information from three dimensional spatial coherence," *J. Opt. Soc. Am. A*, vol. 3, no. 1, pp. 94–100, 1986.

[7] J. Rosen and A. Yariv, "General theorem of spatial coherence: application to three-dimensional imaging," *J. Opt. Soc. Am. A*, vol. 13, no. 10, pp. 2091–2095, 1996.

[8] D. L. Marks, R. A. Stack, D. J. Brady, D. C. Munson, Jr., and R. B. Brady, "Visible cone-beam tomography with a lensless interferometric camera," *Science*, vol. 284, no. 5423, pp. 2164–2166, 1999.

[9] G. Barbastathis, M. Balberg, and D. J. Brady, "Confocal microscopy with a volume holographic filter," *Opt. Lett.*, vol. 24, no. 12, pp. 811–813, 1999.

[10] G. Barbastathis and D. J. Brady, "Multidimensional tomographic imaging using volume holography," *Proc. IEEE*, vol. 87, no. 12, pp. 2098–2120, 1999.

[11] G. G. Yang, H. S. Chen, and E. N. Leith, "Volume reflection holographic confocal imaging," *Appl. Opt.*, vol. 39, no. 23, pp. 4076–4079, 2000.

[12] H.-Y. S. Li, Y. Qiao, and D. Psaltis, "Optical network for real-time face recognition," *Appl. Opt.*, vol. 32, no. 26, pp. 5026–5035, 1993.

[13] M. Levene, G. J. Steckman, and D. Psaltis, "Method for controlling the shift invariance of optical correlators," *Appl. Opt.*, vol. 38, no. 2, pp. 394–398, 1999.

[14] E. N. Leith, A. Kozma, J. Upatnieks, J. Marks, and N. Massey, "Holographic data storage in three-dimensional media," *Appl. Opt.*, vol. 5, no. 8, pp. 1303–1311, August 1966.

[15] G. Barbastathis, M. Levene, and D. Psaltis, "Shift multiplexing with spherical reference waves," *Appl. Opt.*, vol. 35, pp. 2403–2417, 1996.